

Ground Penetrating Radar Fundamentals

by

Jeffrey J. Daniels, Department of Geological Sciences, The Ohio State University

Prepared as an appendix to a report to the U.S.EPA, Region V

Nov. 25, 2000

Introduction

Ground penetrating radar (commonly called GPR) is a high resolution electromagnetic technique that is designed primarily to investigate the shallow subsurface of the earth, building materials, and roads and bridges. GPR has been developed over the past thirty years for shallow, high resolution investigations of the subsurface. GPR is a time-dependent geophysical technique that can provide a 3-D pseudo image of the subsurface, including the fourth dimension of color, and can also provide accurate depth estimates for many common subsurface objects. Under favorable conditions, GPR can provide precise information concerning the nature of buried objects. It has also proven to be a tool that can be operated in boreholes to extend the range of investigations away from the boundary of the hole.

GPR uses the principle of scattering of electromagnetic waves to locate buried objects. The basic principles and theory of operation for GPR have evolved through the disciplines of electrical engineering and seismic exploration, and practitioners of GPR tend to have backgrounds either in geophysical exploration or electrical engineering. The fundamental principle of operation is the same as that used to detect aircraft overhead, but with GPR that antennas are moved over the surface rather than rotating about a fixed point. This has led to the application of field operational principles that are analogous to the seismic reflection method.

GPR is a method that is commonly used for environmental, engineering, archeological, and other shallow investigations. The fundamental principles that are described in the following text applies to all of these applications.

Basic Principles

The practical result of the radiation of electromagnetic waves into the subsurface for GPR measurements is shown by the basic operating principle that is illustrated in Figure A1. The electromagnetic wave is radiated from a transmitting antenna, travels through the material at a velocity which is determined primarily by the permittivity of the material. The wave spreads out and travels downward until it hits an object that has different electrical properties from the surrounding medium, is scattered from the object, and is detected by a receiving antenna. The surface surrounding the advancing wave is called a *wavefront*. A straight line drawn from the transmitter to the edge of the wavefront is called a *ray*. Rays are used to show the direction of travel of the wavefront in any direction away from the transmitting antenna. If the wave hits a buried object, then part of the waves energy is “reflected” back to the surface, while part of its energy continues to travel downward. The wave that is reflected back to the surface is captured by a receive antenna, and recorded on a digital storage device for later interpretation.

Antennas can be considered to be transducers that convert electric currents on the metallic antenna elements to transmit electromagnetic waves that propagate into a material. Antennas radiate electromagnetic energy when there is a change in the acceleration of the current on the antenna. The acceleration that causes radiation may be either linear, (e.g., a time-varying electromagnetic wave traveling on the antenna), or angular acceleration. Radiation occurs along a curved path, and radiation occurs anytime that the current changes direction (e.g. at the end of the antenna element). Controlling and directing the radiation from an antenna is the purpose of antenna design.

Antennas also convert electromagnetic waves to currents on an antenna element, acting as a receiver of the electromagnetic radiation by capturing part of the electromagnetic wave. The *principle of reciprocity* says that the transmit and receive antennas are interchangeable, and this theory is valid for antennas that are transmitting and receiving signals in the air, well above the surface of the ground. In practice, transmit and receive antennas are not strictly interchangeable when placed on the ground, or a lossy material surface, because of attenuation effects of the ground in the vicinity of the transmit antenna.

Electromagnetic waves travel at a specific velocity that is determined primarily by the permittivity of the material. The relationship between the velocity of the wave and material properties is the fundamental basis for using GPR to investigate the subsurface. To state this fundamental physical principle in a different way: the velocity is different between materials with different electrical properties, and a signal passed through two materials with different electrical properties over the same distance will arrive at different times. The interval of time that it takes for the wave to travel from the transmit antenna to the receive antenna is simply called the *travel time*. The basic unit of electromagnetic wave travel time is the nanosecond (ns), where $1 \text{ ns} = 10^{-9} \text{ s}$. Since the velocity of an electromagnetic wave in air is $3 \times 10^8 \text{ m/s}$ (0.3 m/ns), then the travel time for an electromagnetic wave in air is approximately 3.3333 ns per m traveled. The velocity is proportional to the inverse square root of the permittivity of the material, and since the permittivity of earth materials is always greater than the permittivity of the air, the travel time of a wave in a

material other than air is always greater than 3.3333 ns/m. The travel time of an electromagnetic wave through two different materials is shown in Figure A2(a).

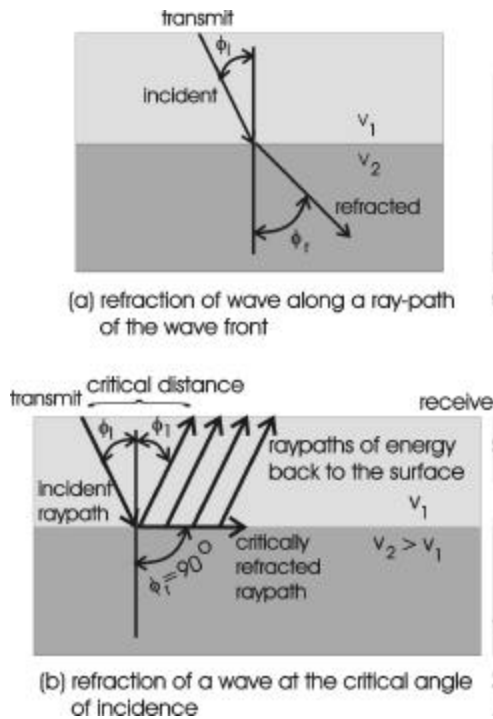


FIGURE A1. Transmitted electromagnetic wavefront scattered from a buried object with a contrasting permittivity. Permittivity of the host media is ϵ_1 , and the permittivity of the buried object is ϵ_2 .

Considering the wave scattered from the object in Figure A1, if a receive antenna is switched-on at precisely the instant that the pulse is transmitted, then two pulses will be recorded by the receive antenna. The first pulse will be the wave that travels directly through the air (since the velocity of air is greater than any other material), and the second pulse that is recorded will be the pulse that travels through the material and is scattered back to the surface, traveling at a velocity that is determined by the permittivity (ϵ) of the material. The resulting record that is measured at the receive antenna is similar to one of the time-amplitude plots in Figure A2(b), with the “input” wave consisting of the direct wave that travels through air, and the “output” pulse consisting of the wave reflected from the buried scattering body. The recording of both pulses over a period of time with receive antenna system is called a “trace”, which can be thought of as a time-history of the travel of a single pulse from the transmit antenna to the receive antenna, and includes all of its different travel paths. The *trace* is the basic measurement for all time-domain GPR surveys. A *scan* is a trace where a color scale has been applied to the amplitude values. The round-trip (or two-way) travel time is greater for deep objects than for shallow objects. Therefore, the time of arrival for the reflected wave recorded on each trace can be used to determine the depth of the buried object, if the velocity of the wave in the subsurface is

known. The principles of constructing a scan from a sequence of traces is shown in Figure A3.

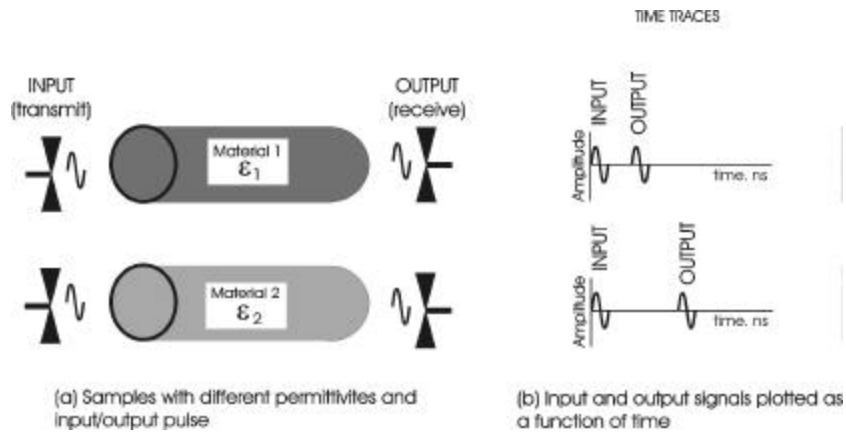


FIGURE A2. Relationship between travel effect of permittivity on travel time through a sample: (a) input and output pulse through samples with different permittivities and velocities, and (b) time versus amplitude plots showing the time differential between the input and output signals for each sample.

The trace is the time-history record (measured in nanoseconds for radar waves) of a tiny piece (in the spatial sense) of a pulse of electromagnetic energy that travels from the transmit antenna and ends up at the receive antenna. If a portion of the wavefront encounters an object with a permittivity different from the surrounding material (host media), then that portion changes direction by a process that is called scattering. Scattering at the interface between an object and the host material is of four main types: 1) specular reflection scattering, 2) diffraction scattering, 3) resonant scattering, and 4) refraction scattering, as shown in Figure A4.

Specular reflection scattering is the common model for the seismic reflection technique. If the transmit and receive GPR antennas separate entities, then the system is called a *bistatic* antenna arrangement. If bistatic GPR antennas are deployed with the transmit and receive antennas located closely together, then the energy that is recorded is often called *back scattered* energy. If the same antenna is used for transmitting and receiving the signal, then the antenna system is called a *monostatic* system. Specular scattering is based on the Law of Reflection, where the angle of reflection is equal to the angle of incidence, or $\phi_1 = \phi_2$ in Figure A4(a).

When a wave impinges on interface, it scatters the energy according to the shape and roughness of the interface and the contrast of electrical properties between the host material and the object. Part of the energy is scattered back into the host material, while the other portion of the energy may travel into the object. The portion of the wave that propagates into the object is said to be refracted. The angle that the wave enters into the object is determined by Snell's law, which can be stated as follows:

$$\frac{v_1}{v_2} = \frac{\sin \phi_1}{\sin \phi_2} \quad (1)$$

where v_1 and v_2 are the velocities of the wave through the upper and lower materials, respectively, and ϕ_1 and ϕ_2 are the angles of the raypath for the incident and refracted waves, respectively.

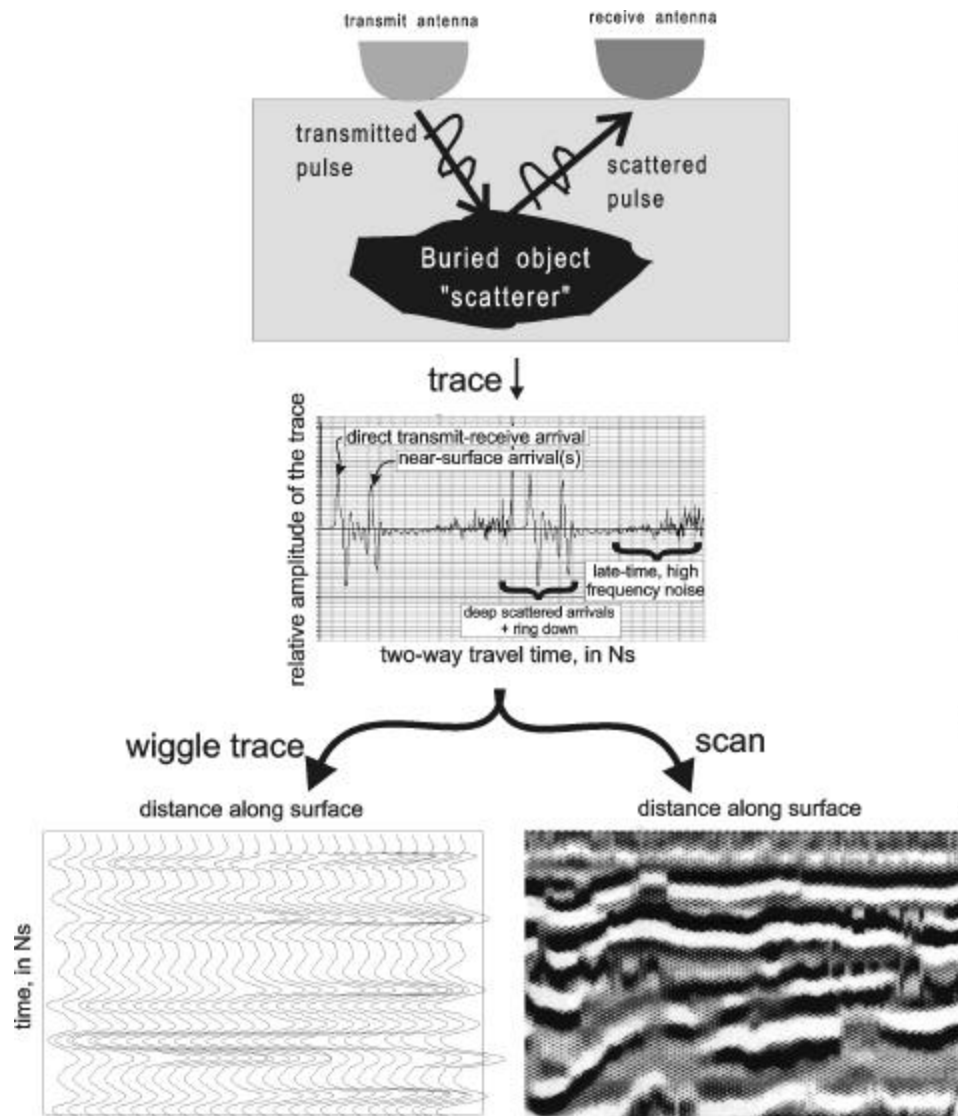


FIGURE A3. The process of constructing a scan from a series of traces measured along the surface. Sequence of producing a GPR profile: 1. transmit and receive electromagnetic energy, 2. the received energy is recorded as a trace at a point on the surface, 3. traces are arranged side-by-side to produce a cross section of the earth recorded as the antennas are pulled along the surface. Traces are displayed as either wiggle trace, or scan plots (gray scale or color assigned to specific amplitudes).

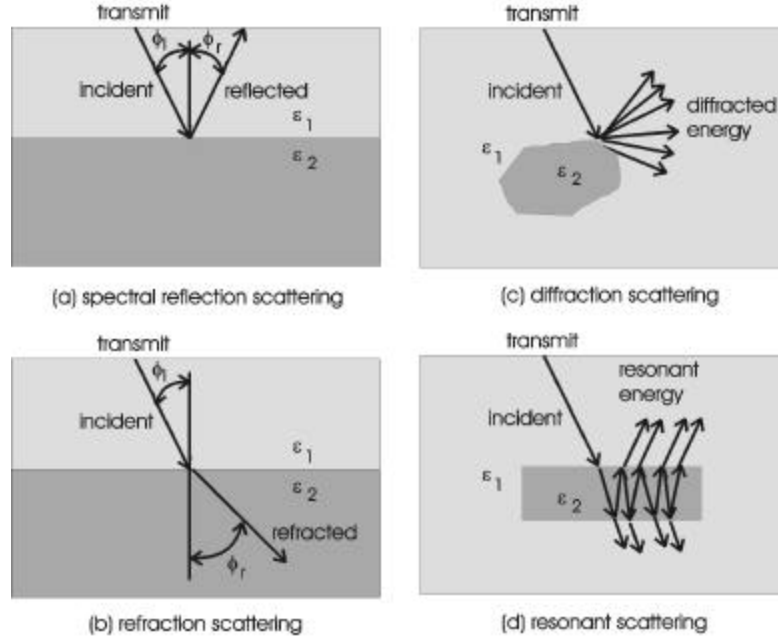


FIGURE A4. Scattering mechanisms: (a) specular reflection scattering, (b) refraction scattering, (c) diffraction scattering, and (d) resonant scattering.

If the interface is smooth and continuous (e.g., a layer boundary), and velocity of the wave in the lower boundary (e.g., the object, or lower layer) is greater than velocity in the host material, then the wave within the object we'll travel along the interface with a velocity that is equal to velocity of wave in the object. The angle where this occurs is called critical angle, and can be determined by the following equation:

$$\frac{\sqrt{\epsilon_2}}{\sqrt{\epsilon_1}} = \frac{v_1}{v_2} = \sin \phi_1 \quad (2)$$

The distance that the receiver must be from the transmitter to receive a refracted wave is called the critical distance. Refracted waves are uncommon as a propagation path for GPR, since the electromagnetic wave velocity tends to decrease with depth. This is a consequence of the fact that seismic and electromagnetic wave velocities in partially saturated and unconsolidated materials are affected primarily by the water content.

Diffraction (Figure A4-c) is the bending of electromagnetic waves. Diffraction scattering occurs when a wave is partially blocked by a sharp boundary. Huygen's Principle of spherical spreading applies, but since the wave scatters off of a point, the wave spreads out in different directions, as first noted by Fresnel (1788-1827). The nature of the diffracted energy depends upon the sharpness of the boundaries and the shape of object relative to the wavelength of the incident wave. Diffractions commonly can be seen on GPR data as semi-coherent energy patterns that splay out in several directions from a point, or a along

a line. Geologically, they often are measured in the vicinity of a vertical fault, or a discontinuity in a geologic layer (abrupt facies change).

Resonant scattering occurs when a wave impinges on a closed object (e.g., a cylinder), and the wave bounces back-and-forth between different points of the boundary of the object. Every time the wave hits a boundary, part of the energy is refracted back into the host material, and part of the energy is reflected back into the object. This causes the electromagnetic energy to resonate (sometimes called ringing) within the object. The resonant energy that is trapped inside of the object quickly dissipates as part of it is re-radiated to the outside of the object. Closed objects are said to have a resonant frequency that is based on the size of the object, and the electrical properties of the object and the surrounding material. However, the ability of an object to resonate depends on the wavelength (velocity of the object, divided by the frequency of the wave) with respect to dimensions of the object. The length of time that an object resonates is determined by the permittivity contrast between the object and the surrounding material.

In practice, GPR measurements can be made by towing the antennas continuously over the ground, or at discrete points along the surface. These two modes of operation are illustrated in Figure A5. The fixed-mode antenna arrangement consists of moving antennas independently to different points and making discrete measurements, while moving-mode keeps the transmit and receive antennas at a fixed distance with the antenna pair moved along the surface by pulling them by hand, or with a vehicle. The fixed-mode arrangement has the advantage of flexibility, moving-mode has the advantage of rapid data acquisition. In practice, a combination of fixed-mode and moving-mode provides an optimum mixture of flexibility and mobility. Measurements made in the fixed mode can be used to determine the best spacing and antenna orientation for making moving mode measurements. Some systems enable the operator to make both types of measurements with the same antennas and electronics.

GPR Field Systems

The transmit and receive antennas are moved independently in the fixed mode of operation. This allows more flexibility of field operation than when the transmit and receive antennas are contained in a single box. For example, different polarization components can be recorded easily when the transmit and receive antennas are separate. In the fixed-mode of operation, a trace is recorded at each discrete position of the transmit and receive antennas through the following sequence of events in the GPR system: 1) a wave is transmitted, 2) the receiver is turned on to receive and record the received signals, and 3) after a certain period of time the receiver is turned off. The resulting measurements that are recorded during the period of time that the receiver is turned on is called a trace, as described earlier. Figure A5(a) shows a trace in over a single layer. The idealized trace for this simple case consists of a direct pulse, and a single reflection from the layer.

In the moving mode of operation, a radar wave is transmitted, received and recorded each time that the antenna has been moved a fixed distance across the surface of the ground, or material, that is being investigated. Since a single record of a transmitted pulse is called a trace, the spacing between measurement points is called the *trace spacing*. The trace spac-

ing that is chosen should be a function of the target size and the objectives of the survey. A single trace over two layers is shown in Figure A5(a). Traces that are displayed side-by-side form a *GPR time-distance record*, or *GPR cross section*, which shows how the reflections vary in the subsurface. If the contrasts in electrical properties (e.g. changes in permittivity) are relatively simple, then the GPR time-distance record can be viewed as a two-dimensional pseudo-image of the earth, with the horizontal axis the distance along the surface, and the vertical axis being the two-way travel time of the radar wave. The two-way travel time on the vertical axis can be converted to depth, if the permittivity (which can be converted to velocity) is known. The GPR time-distance record is the simplest display of GPR data that can be interpreted in terms of subsurface features. A GPR time-distance record can also be produced by making a series of fixed-mode measurements at a constant interval between traces on the surface.

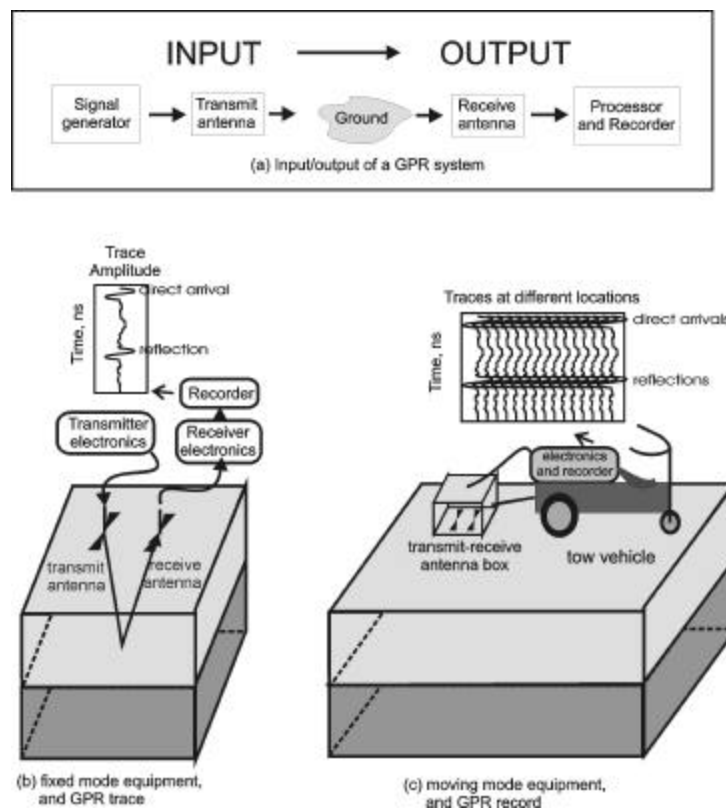


FIGURE A5. Fixed and continuous mode GPR operation on the surface. The primary electronics may be mounted on the antennas, in the antenna box, or in a box that is separate from the antennas. The transmit pulser is usually located in close proximity to the transmit antenna element. (a) fixed mode produce a trace, (b) moving mode produces a GPR time-distance record.

GPR equipment consists of antennas, electronics and a recording device, as shown in Figure A5(b). The transmitter and receiver electronics are always separate, but in a fixed-mode configuration, they are often contained in different boxes, while in some systems that are designed for moving-mode operation, all of the electronics are contained in one box. In some cases, the electronics may be mounted on top of the antennas, which makes for a compact system, but it also decreases the operational flexibility of the system.

GPR systems are digitally controlled, and data are usually recorded digitally for post-survey processing and display. The digital control and display part of a GPR system generally consists of a micro-processor, memory, and a mass storage medium to store the field measurements. A small micro-computer and standard operating system is often utilized to control the measurement process, store the data, and serve as a user interface. Data may be filtered in the field to remove noise, or the raw data may be recorded and the data processed for noise removal at a later time. Field filtering for noise removal may consist of electronic filtering and/or digital filtering prior to recording the data on the mass data storage medium. Field filtering should normally be minimized except in those cases where the data are to be interpreted immediately after recording.

Data Display and Interpretation

The objective of GPR data presentation is to provide a display of the processed data that is closely approximates an image of the subsurface, with the anomalies that are associated with the objects of interest located in their proper spatial positions. Data display is central to data interpretation. In fact, producing a good display is an integral part of interpretation.

There are three types of displays of surface data, including: 1) a one-dimensional trace, 2) a two dimensional cross section, and 3) a three dimensional display. Borehole data can be displayed as a two-dimensional cross section, or processed to be displayed as a velocity tomogram. A one-dimensional trace is not of very much value until several traces are placed side-by-side to produce a two dimensional cross section, or placed in a three dimensional block view.

The wiggle trace (or scan) is the building block of all displays. A single trace can be used to detect objects (and determine their depth) below a spot on the surface. By towing the antenna over the surface and recording traces at a fixed spacing, a record section of traces is obtained. The horizontal axis of the record section is surface position, and the vertical axis is round-trip travel time of the electromagnetic wave. A GPR record section is very similar to the display for an acoustic sonogram, or the display for a fish finder. Two types of wiggle-trace cross-sections of GPR traces are shown in Figure A6. Wiggle trace displays are a natural connection to other common displays used in engineering (e.g., and oscilloscope display), but it is often impractical to display the numerous traces that are measured along a GPR transect in wiggle-trace form. Therefore, scan displays have become the normal mode of two dimensional data presentation for GPR data. A scan display is obtained by simply assigning a color (or a variation of color intensity) to amplitude ranges on the trace, as shown in Figure A6-a. Two forms of scan data are shown in Figure A6, including: a) a gray-scale display ranging from black to white, and b) a color intensity display using a single color ranging from white (or black) to the pure form of the color.

Three dimensional displays are fundamentally block views of GPR traces that are recorded at different positions on the surface. Data are usually recorded along profile lines, in the case of a continuous recording system (see Figure A7), or at discrete points on the surface in fixed-mode recording. In either case, the antennas must be oriented in the

same polarization orientation direction for each recording position if linearly polarized dipole antennas are used.

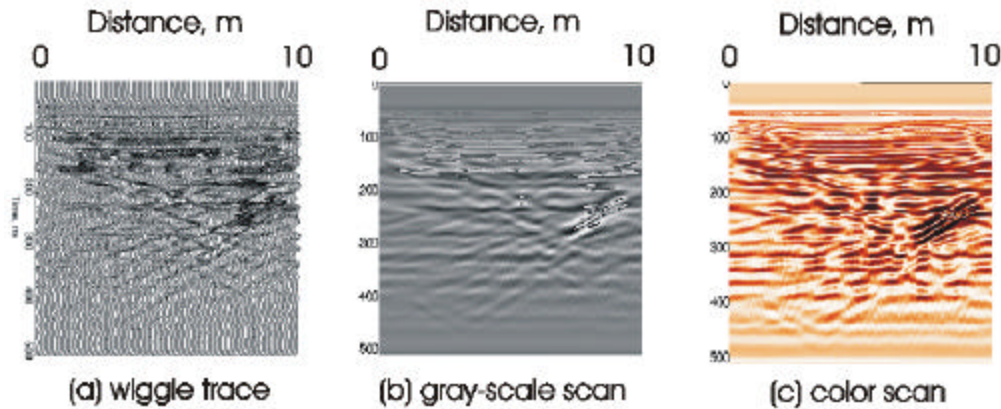


FIGURE A6. Scan displays: a) the conversion of a wiggly trace display to a color scan display, b) a gray scale scan display, c) a color intensity scan display.

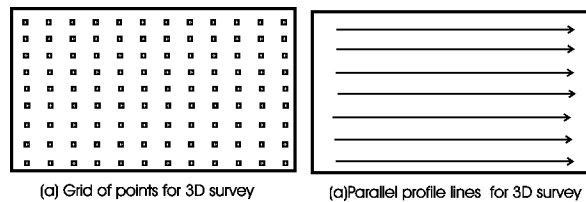


FIGURE A7. Grids and lines for fixed-mode and moving-mode for three-dimensional data measurements. Note that the polarization orientation of the antennas is the same for each measurement point on the grid, or along the profile lines.

The typical transmit-receive antenna configuration for three dimensional display is for the antennas to be located the same distance apart for each measurement on the surface. If the antennas are placed together as closely as possible for each measurement point, then this is called coincident antenna three dimensional ground penetrating radar (GPR) measurement mode. Measurements may be made using antennas that are towed behind a vehicle, or in a fixed-station (fixed-trace) mode of operation. In either case, the accurate location of each trace is critical to producing accurate 3D displays. Normally 3D block views are constructed from several parallel, closely spaced lines, as shown in Figure A8. Once the blocks are constructed, then they may be viewed in a variety of ways, including as a solid block or as block slices, as shown in Figure A9.

Obtaining a good three dimensional display is a critical part of interpreting GPR data. Targets of interest are generally easier to identify and isolate on three dimensional data sets than on conventional two dimensional profile lines. Simplifying the image, by eliminating

the noise and clutter is the most important factor for optimizing the interpretation. Image simplification may be achieved by: 1) carefully assigning the amplitude-color ranges, 2) displaying only one polarity of the GPR signal, 3) using a limited number of colors, 4) decreasing the size of the data set that is displayed as the complexity of the target increases, 5) displaying a limited time range (finite-thickness time slice) and 6) carefully selecting the viewing angle. Further image simplification in cases of very complex (or multiple) targets may also be achieved by displaying only the peak values (maximum and minimum values) for each trace. Finite-thickness (pillow) time slices and cross sections have many advantages over the infinitesimal thin slices that are routinely used for interpreting GPR data. Examples of sub-blocks that can help to isolate anomalies are shown in Figure A10.

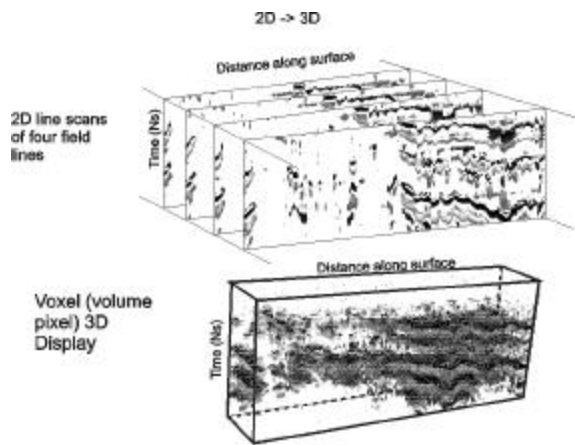


FIGURE A8. The process of constructing a three-dimensional display from a series of two-dimensional lines: a) series of two-dimensional lines, and b) three dimensional block view.

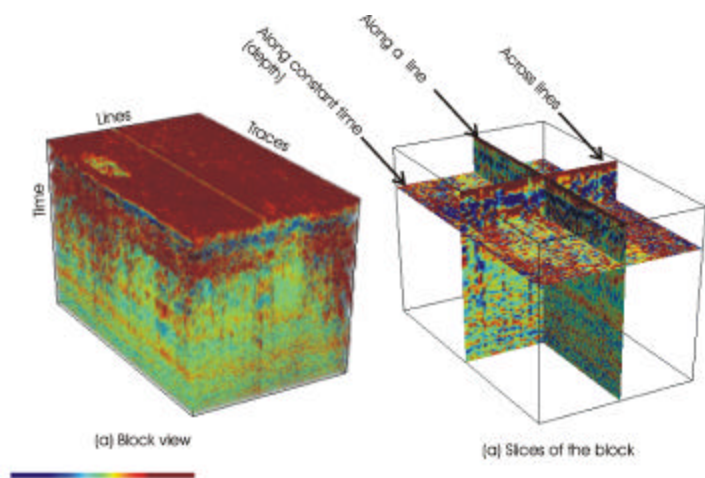


FIGURE A9. Dissecting a three-dimensional block into slices.

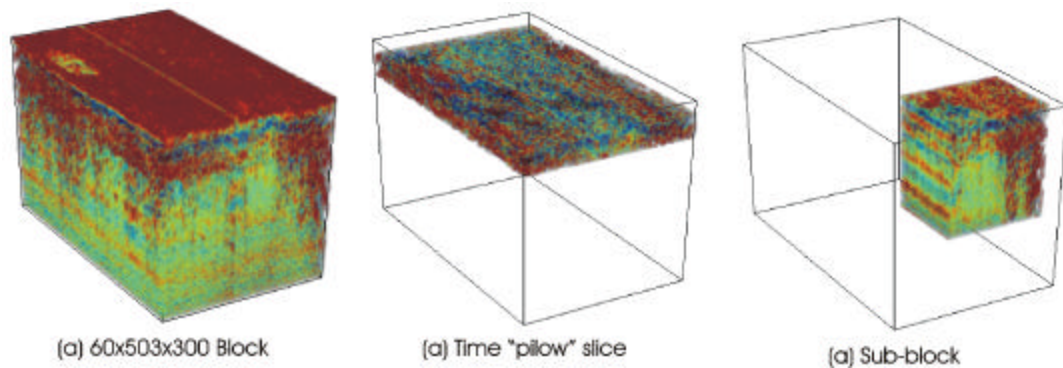


FIGURE A10. Block and sub-block views to focus on a particular region inside of a block.

3D GPR Data Application

A detailed Ground Penetrating Radar Survey was conducted at two locations on the Brookhaven National Laboratory property to locate and define the size and depth of pits containing laboratory waste. The two sites were named the “Glass Hole Area”, and the “Animal/Chemical Pit Area”. The location map for the two sites is given in Figure A11. The areas contained mounds of dirt, and were overgrown with weeds and evergreen trees. The vegetation and mounds of dirt made it logistically impossible to obtain good geophysical measurements, so the trees were removed and each area was leveled with a bulldozer before making geophysical measurements on the surface of the site. Detailed magnetic gradients, three types of inductive electromagnetic surveys were made in addition to two GPR surveys (linear dipole and circularly polarized antenna systems). The magnetic and electromagnetic surveys were used as a first-order estimate on the location of the pits containing metallic objects. However, a few of the pits did not contain any metallic waste, and these pits could only be detected with GPR. Also, the GPR was used to define the lateral boundaries of the pits, which was not possible with the magnetic and electromagnetic methods.

A sandy glacial till is present at the surface. From a geophysical perspective, the unconsolidated sandy till is relatively homogenous, with radar penetration depths at 80 Mhz that are greater than 12 m. Cores and outcrops show some stratification within the till that is primarily a variation in grain size, and this subtle layering is clearly seen on the GPR displays. The water table is at a depth of approximately 12 m throughout the site, and is clearly visible as a strong scattering layer on the GPR data displays. Velocities determined from diffraction hyperbolas are consistently 0.12 m/Ns for each of the two survey areas, and this velocity is consistent with the two-way travel time from the known water-table reflection.

Detailed surface GPR surveys were made at two sites over the areas shown in Figure A11. A conventional 80 MHz linear dipole antenna was towed behind an All Terrain Vehicle for the measurements discussed in this paper. The data were digitally recorded at a trace spacing along the lines of 0.1 m, and a spacing between lines of 0.5 m. High spatial data

density is critical to obtaining an accurate 3D presentation of the data. The location of individual traces along the traverse (or profile) lines were carefully controlled by a distance wheel that triggered the recording of a trace every 0.1 m along the line. Typically, 495 to 505 traces were recorded along lines that were 50 m long. The variation in the number of traces per unit distance caused a cumulative distance error along the line of less than 1 percent. Since the cumulative error increased as a function of line length, lines were restricted to a distance of less than 50 meters at the Animal/Chemical Pit Area and less than 67 m at the Glass Hole Area. A mark was chalked on the surface for each line prior to GPR surveying to insure an accurate spacing between traverse lines.

Processing of 2D cross sections consisted simply of band-pass frequency filtering from 50 to 700 MHz to remove the low frequency bias from the traces. Data samples from the cross sections were placed directly into a three dimensional matrix (consisting of 1 byte samples) for display. The principles illustrated in this paper can be reproduced with any volumetric pixel based display program on many different types of hardware platforms. The volumetric pixel display (sometimes referred to as a voxel display) displays each data point directly, without interpolating between points to fit a polygonal surface to the data. All displays in this paper use data that has been processed to eliminate everything except the peak values on each trace, preserving only the maximum values (Daniels and others, 1997). Maximum amplitude processing sharpens the 3D displays by eliminating transitional data points between the peak values. In addition, displaying only a single polarity further simplifies the data display, and improves the definition of individual anomalies within complex groups of anomalies.

The objective of the BNL GPR surveys was to provide accurate locations of the boundaries of the pits, and details concerning the amount of material in each pit. This objective would have been difficult to achieve without using the 3D data. The objectives required a threefold approach: 1) determine the location of each pit, 2) verify the presence of the pit with 3D views, and 3) determine the depth and distribution of objects within the pits using detailed 3D views. It was determined during the course of this investigation that there is no simple way to achieve these objectives. The objectives were achieved by a slow interpretive investigation of each pit. The choice of optimum amplitude range that was displayed varied from pit-to-pit. Hence, the choice of display parameters was an integral part of the interpretation process.

The final interpreted lateral positions and outlines of the pits are given in Figure A11, and the time slice plan views of the GPR data are shown in Figure A12. In some cases the pits are isolated and their positions are obvious from the time slice information. This is particularly true for pits G3 and G4 in the Glass Hole Area, and pits C18 and C8 in the Animal/Chemical pit area. However, in other cases the time slice data does not provide enough information to positively locate the pit and the pit boundaries. This is the usual situation when the pits are very close together, such as the group of pits on the southeast side of the Glass Hole Area. In these situations, it is necessary to scan the 3D block views in order to isolate the pits.

The 3D block view for pit G2 in the Glass hole area is shown in Figure A13, along with the in-line cross section. The in-line cross section (Figure A13a) does highlight the pit and

other features around the pit. However, the in-line cross section has at least two major shortcomings for interpretation, including: 1) the in-line cross section registers scattering events from objects that are perpendicular from the in-line traverse, and 2) parallel in-line traverses must be investigated individually to define the subsurface object. The comparison of adjacent in-line traverses is a cumbersome time-consuming task that is error-prone.

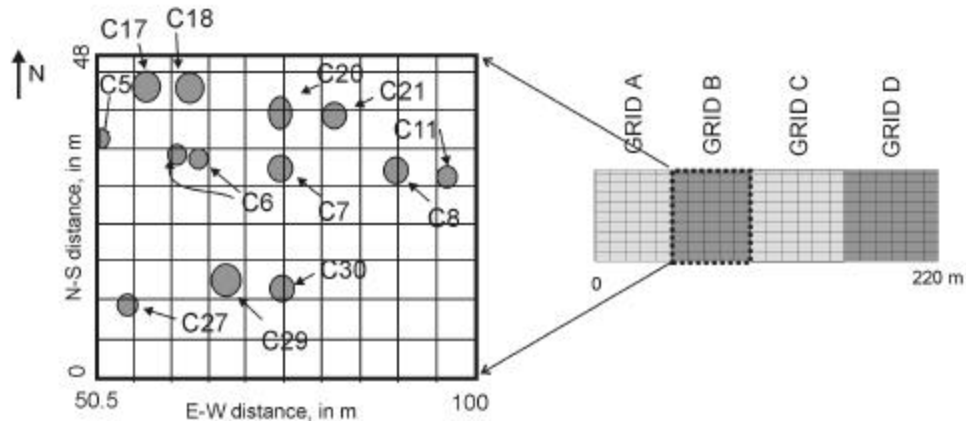
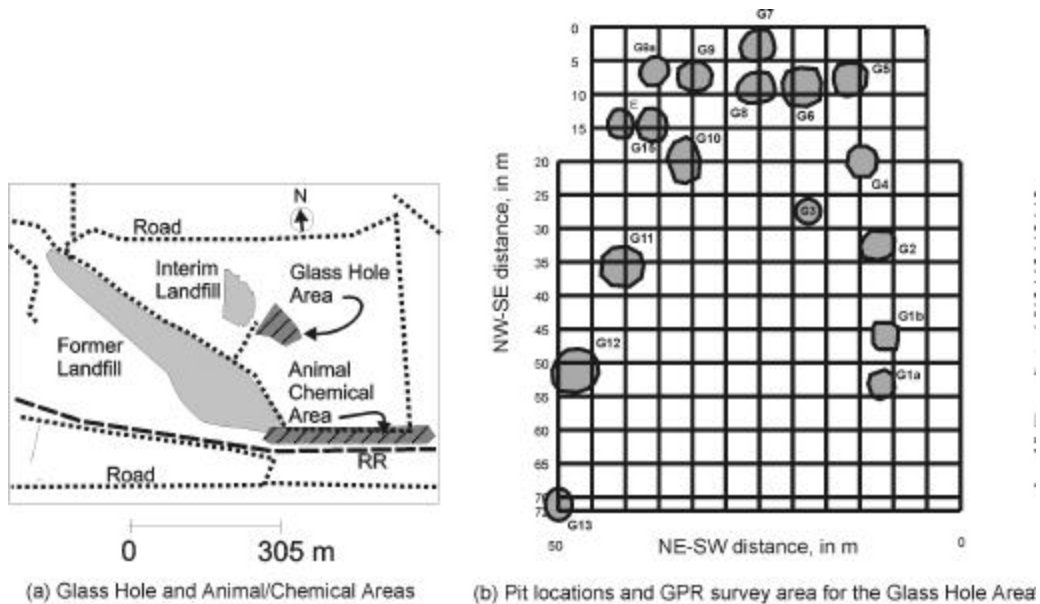


FIGURE A11. Pit locations for the Glass Hole area and Grid B in the Animal/Chemical Pit area of Brookhaven National Laboratory. (modified from Daniels, et.al., 1998)

The 3D block views for pit G2 (Figures 13-b, and 13-c) provide a positive identification of the pit, and can immediately be used to verify the lateral location of the pit. In those cases where there is a shallow near-surface layer, such as pit G2, the hole that was dug through the layer can be clearly seen on the 3D block view. In many cases the base of the pit can be clearly identified on the 3D block view. This is not the case for pit G2 shown in Figure A13, where the waste appears to be continuous to depths beyond practical burial limits. The apparent deep extension of the waste may be caused by ringing events on the GPR

record from metallic objects within the pit. The ability to define the contents of the pit depends upon the nature of the waste contained in the pit.

A detailed time-slice view of the pits in the northern portion of Grid B at the Animal/Chemical pit area is shown in Figure A14. This detailed view provides a better definition of the pits than the broad view shown in Figure A12. The lateral boundaries of Pit C8 are defined on the time-slice in Figure A14, and is clearly seen on both the 2D cross section and the 3D block views in Figure A15. The top and bottom of the pit is evident on the 3D view (Figure A15-b), but it is not as obvious on the 2D cross section (Figure A15-a). A close inspection of the 2D cross section shows that the energy scattered from the objects in the pit interfere with the energy from the horizontal interface at the layer boundary, complicating the 2D cross section and making it nearly impossible to identify the bottom of the pit. However, the 3D image clearly shows the depth extent of the coherent high amplitude energy.

Data for Pit C11 illustrates a situation where the pit is difficult to identify from the chosen time-slice (Figure A14), but the pit is clearly shown on the 3D view, as seen in Figure A16. There is simply no scattered energy from objects within pit C11 that occurs during the period of the time-slice displayed in Figure A13, but there is enough scattered energy at earlier and later time to form the 3D block views shown in Figure A16. The block view of pit C11 is complicated by the fact that the pit is relatively small, and the scattered energy has a low amplitude when compared to some of the other pits in the Animal/Chemical Pit Area. It can be argued from these examples that the 3D view also provides a truer picture of the subsurface reflections than as series of 2D cross sections. This is partially due to the way that alpha-rendering of 3D voxel data works on variable amplitude data, and partially due to the amplitude assignment values selected by the interpreter. Alpha-rendering is a common means of displaying 3D data so that there is some apparent “transparency” to the image, while producing a minimum amount of distortion of the original data. The final image is biased in favor of the higher amplitude data, which consists primarily of the directly scattered energy.

Conclusions

GPR has been developed into a sophisticated technique that can provide detailed images of the near surface. Most of the research on GPR has been conducted for environmental and engineering applications. However, all of the development in these areas has applications for archeological site characterization and engineering applications. GPR has two advantages over most other non-invasive geophysical techniques: 1) GPR provides a three dimensional pseudo-image that can easily be converted to depths that are accurate down to a few centimeters, and 2) GPR responds to both metallic and non-metallic objects. GPR is an excellent tool for mapping nearly any inhomogeneity in the subsurface that is characterized by a small difference in density, or porosity.

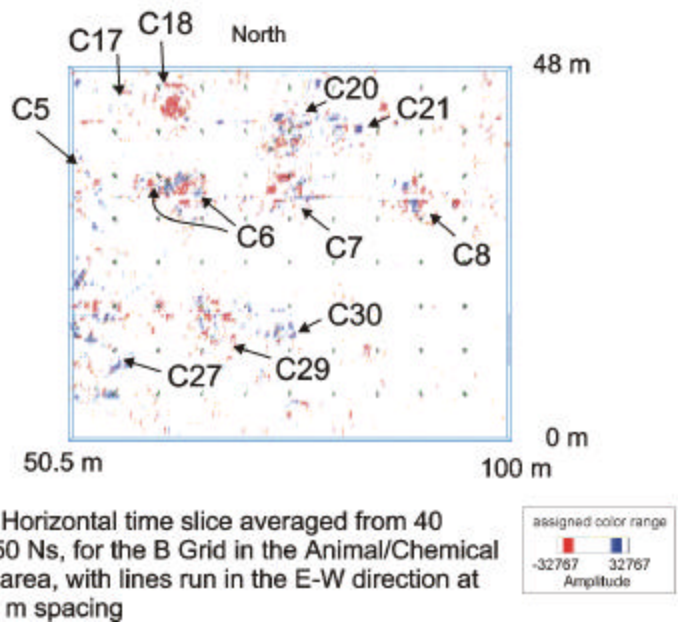
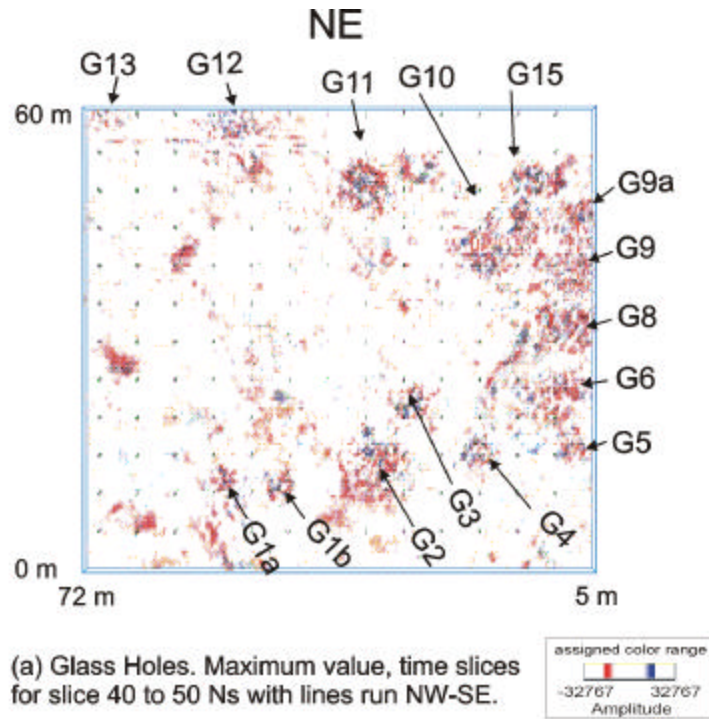


FIGURE A12. Time-slice plan views for the surface GPR data for: (a) the Glass Hole area, and (b) the Animal/Chemical Pit area. (modified from Daniels, et.al., 1998)

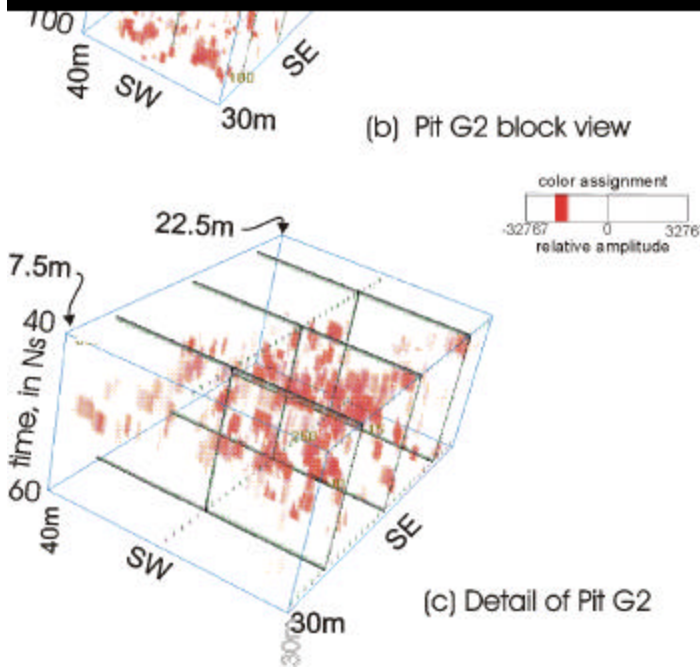
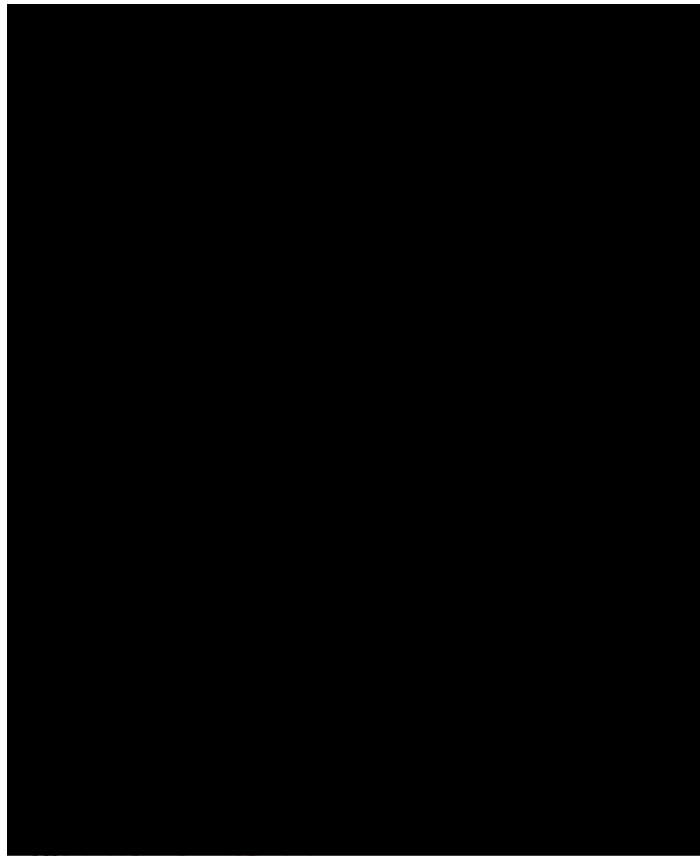


FIGURE A13. Views of pit from GPR data: (a) inline slice, (b) 3D block view, and (c) 3D detailed view. Data from lines run in the SW-NE direction. The top and bottom of the waste is indicated by the symbols “TW”, and “BW”, respectively. (modified from Daniels, et.al., 1998)

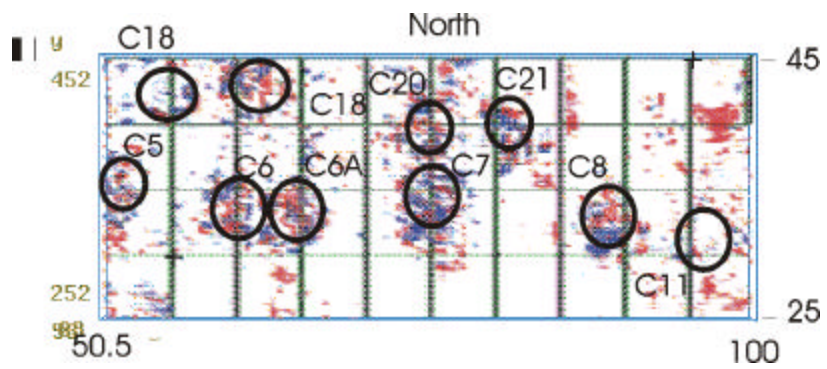
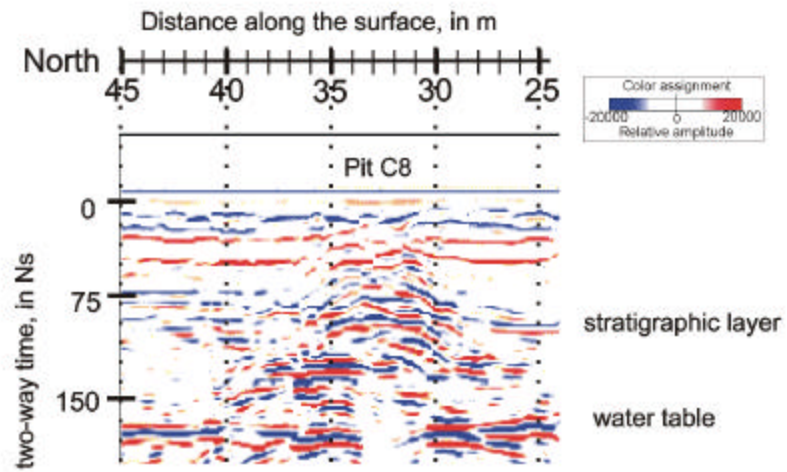
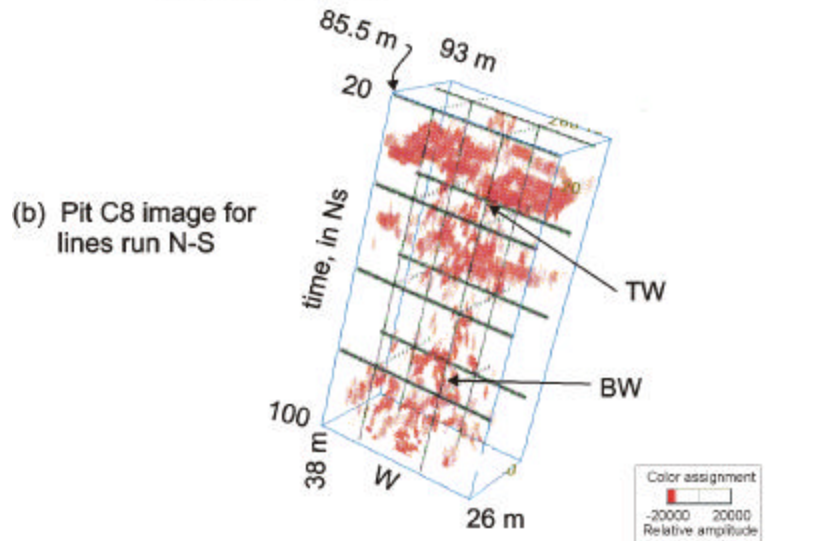


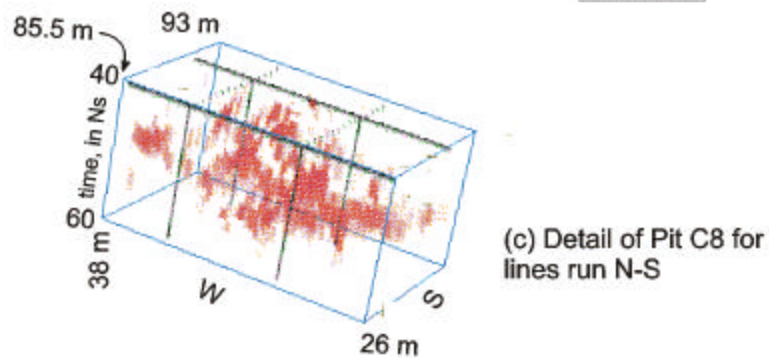
FIGURE A14. Time slice plan view for pits, including pits C8 and C11 locations. (modified from Daniels, et.al., 1998)



(a) North-South surface GPR line along the 87m line.

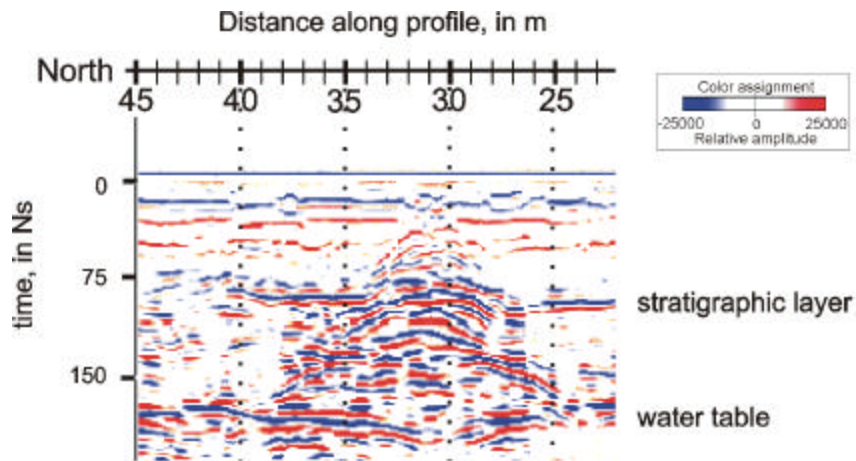


(b) Pit C8 image for lines run N-S



(c) Detail of Pit C8 for lines run N-S

FIGURE A15. Views of C8 pit from GPR data: a) cross section, b) 3D block view, c) 3D detailed view. Interpreted top and bottom of the waste pit are designated by the initials “TW” and “BW”, respectively. (modified from Daniels, et.al., 1998)



(a) North-South surface GPR line along 94 meter line.

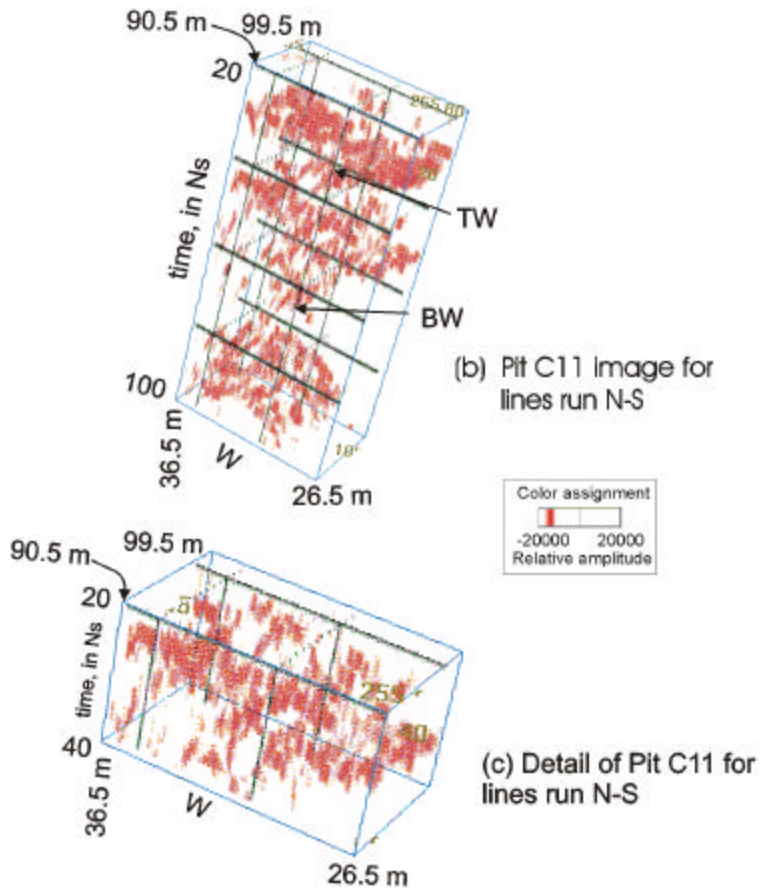


FIGURE A16. Views of C11 pit from GPR data: a) cross section, b) 3D block view, c) 3D detailed block view. Interpreted top and bottom of the waste pit are designated by the initials “TW”, and “BW”, respectively. (modified from Daniels, et.al., 1998)

References

Daniels, J.J., Grumman, D., and Vendl, M., 1997, Vertical Incident Three Dimensional GPR: *Jour. Env. Eng. Geoph.*, V. 2, No. 2, p. 1-9.

Daniels, J.J., Brower, J., and Baumgartner, F., 1998, High resolution GPR at Brookhaven National Laboratory to delineate complex subsurface targets: *Journal of Environmental and Engineering Geophysics*, Vol. 3, No. 1, p. 1-5.